

^{195}Pt spin dynamics and Knight shift in single crystals of UPt_3

Moohee Lee,* G. F. Moores, Y.-Q. Song, and W. P. Halperin

Department of Physics and Astronomy and Materials Research Center, Northwestern University, Evanston, Illinois 60208

W. W. Kim and G. R. Stewart

Department of Physics, University of Florida, Gainesville, Florida 32611

(Received 23 December 1992; revised manuscript received 29 March 1993)

^{195}Pt nuclear-magnetic-resonance measurements were performed on aligned single-crystal whiskers of UPt_3 for temperatures from 4 to 50 K. A special alignment technique allows us to produce samples with very good c -axis alignment and to work with the field parallel to the c axis with an excellent signal-to-noise ratio. Combining the Knight shift and spin-lattice-relaxation data, we show a continuous crossover from paramagnetic behavior above 40 K toward a degenerate-Fermi-liquid behavior below 5 K. Antiferromagnetic spin fluctuations appear to be responsible for this crossover process, and dominate all low-frequency magnetic properties of this compound. The anisotropy ratios of both the spin-lattice and the spin-spin relaxation rates are found to be temperature independent. Analyzing these ratios we find that the imaginary part of the dynamic spin susceptibility is slightly stronger in the basal plane.

I. INTRODUCTION

Heavy-fermion systems have attracted considerable attention since they exhibit unusual physical properties and a variety of ordered states at low temperature.¹ For example, in UPt_3 , superconductivity²⁻⁴ is found to coexist with antiferromagnetism as inferred from neutron-scattering experiments.⁵ The static antiferromagnetic order is reported to set in below 5 K. Other neutron-scattering experiments^{6,7} have revealed the presence of spin fluctuations at higher temperatures. Short-range antiferromagnetic (AFM) correlations were observed between uranium atoms in adjacent basal planes, as were ferromagnetic (FM) correlations between uranium atoms in the same basal plane.⁷ These correlations are thought to be responsible for the formation of a coherent electronic state leading to a degenerate Fermi-liquid regime.³ In light of the possible significance of antiferromagnetic coupling in the superconducting pairing mechanism,⁸ it is important to study the temperature region where the crossover to the Fermi-liquid behavior occurs.

Nuclear magnetic resonance (NMR) has been an important probe of electronic structure and the low-energy excitations of heavy-fermion metals through the measurements of Knight shift, spectrum linewidth, and nuclear-spin relaxation rates. However, ^{195}Pt NMR on a powder sample of UPt_3 is difficult to interpret due to the enormous broadening from Knight shift anisotropy.^{9,10} We have discovered a way to align the UPt_3 whiskers, each of which is a high-quality single crystal, and we have measured anisotropic Knight shifts and relaxation rates in a temperature range of 4–50 K. These measurements show a continuous crossover from paramagnetic behavior above 40 K toward a degenerate Fermi-liquid behavior below 5 K.

II. SAMPLE PREPARATION AND MEASUREMENTS

Single-crystal whiskers were grown by a method reported previously.² The whiskers were less than 40 μm thick and their principal geometric axis is the crystalline c axis. The small thickness of the whiskers allows complete rf penetration at our NMR frequency of 11 MHz throughout the measurement temperature range. The superconducting onset temperature and the transition width were measured for several whiskers to be typically 0.5 and 0.01 K, respectively. The residual resistance ratio, defined as the ratio of the room-temperature resistance to the resistance at the superconducting transition temperature, was measured for one whisker to be 100.

The alignment of the c axis of the whiskers was achieved by *rotating the whiskers*, contained in a cylindrical glass tube, *in a magnetic field*, with the rotation axis perpendicular to the field. For UPt_3 , the magnetic susceptibility is largest when the field is in the basal plane. Therefore, a static magnetic field, without additional rotation, will bring the c axis of the whiskers into a plane perpendicular to the field. The c axis is randomly oriented in this plane. This degeneracy can be lifted by a rotation, perpendicular to the field, which tilts the c axis of the whiskers out of the plane. The only equilibrium configuration is the c axis coinciding with the rotation axis and thus perpendicular to the field.

UPt_3 whiskers were mixed in a diluted resin (nail polish diluted in acetone) and rotated at a speed of 60 revolutions per minute in a magnetic field of 10 KG until the resin was dry. The magnetic field was horizontal and perpendicular to the rotation axis. An almost horizontal rotation axis is chosen to avoid premature sedimentation. Due to the huge magnetization anisotropy, the whiskers aligned quickly and then coalesced in the end of the glass

tube. Their alignment was found to be within a half-width of 5° , determined from NMR linewidth analysis described later. Sample *A*, prepared by this method and consisting of thousands of small whiskers, has a dimension $4 \times 2 \times 5 \text{ mm}^3$ and weighed 70 mg. Sample *B*, 13 mg, was prepared by manual alignment of 90 of the largest whiskers we were able to grow, typically 4–10 mm long. The alignment is considered to be within 1° , much better than sample *A*. ^{195}Pt NMR measurements were performed mainly on sample *A*.

The samples were placed in a continuous flow cryostat (Oxford CF200) and the temperature was measured and maintained to an accuracy of $\pm 0.1 \text{ K}$ from 4 to 50 K. The NMR data were taken on a home-built pulsed spectrometer.¹¹ The spurious signal from the strong rf pulses was canceled by alternating the rf phases of both $\pi/2$ and π pulses in the spin echo sequence. In the relaxation measurements, echo sequences with different delay times between pulses were executed consecutively. The whole sequence, including variable pulse separations, was repeated for signal averaging. Such a pulse sequence¹² eliminates long time drifts such as present in electronic amplifier gain and improves measurements of relaxation profiles. The $\pi/2$ pulse length was calibrated with a metallic Pt sample and was typically $1.5 \mu\text{s}$. The spin-lattice relaxation time T_1 was measured by the inversion-recovery method. Measurements were performed in a temperature range of 4–50 K in an external field of 13–14 kG. A metallic ^{63}Cu signal, having a Knight shift of 0.24% in this temperature range,¹³ was used as a reference for Knight-shift measurements. The coil and sample geometry allowed continuous rotation of the sample *c* axis relative to the magnetic field at low temperature. It is straightforward to find the orientation of the whiskers that is perfectly perpendicular to the field using the anisotropy of the Knight shift as a guide. This position is used as the reference for the sample orientation.

We found that eddy current heating of the sample could be significant at the lowest temperature owing to the large rf pulses which we have used. This was observed both from a direct measurement of the sample temperature with a carbon glass temperature sensor, and from the changes of ^{195}Pt frequency as the repetition rate of rf pulses varies. We reduced this heating by shielding the sample with thin copper wires, which were thermally anchored to a heat sink. Furthermore, the repetition time was set long enough (up to 1 s) to ensure that the heating effect was negligible. Throughout our measurements, the temperature rise was less than 0.1 K.

III. ANGULAR DEPENDENCE AND ALIGNMENT ANALYSIS

A typical ^{195}Pt NMR spectrum for $H \perp c$ is shown in the inset of Fig. 1. The spectral linewidth of our aligned single-crystal whiskers, defined as the full-width-at-half-maximum (FWHM), is very narrow, $\sim 50 \text{ kHz}$. Compared to this result, the linewidth of a powder sample¹⁴ is broadened by a factor of 20, to $\sim 1 \text{ MHz}$ at the NMR frequency of 11 MHz.

The angular dependence of the Knight shift was measured at 4.94 K and 12.46 kG [Fig. 1(a)]. As expected for a uniaxial susceptibility,¹⁵ we found that $K(\theta)$ is precisely a linear function of $(3 \cos^2\theta - 1)$, where θ is the angle between the field and the *c* axis. The narrow linewidth of our sample allows small experimental error, typically $\pm 0.1\%$, approximately the size of a data point in Fig. 1(a). We fit the angular dependence of the Knight shift to the form:

$$K(\theta) = (2K_{\perp} + K_{\parallel})/3 + (K_{\parallel} - K_{\perp})(3 \cos^2\theta - 1)/3. \quad (1)$$

The fit is shown in Fig. 1(a). The Knight shifts are large and highly anisotropic: $K_{\parallel} = -1.8\%$ and $K_{\perp} = -9.0\%$ at 4.94 K. Therefore, imperfect alignment results in an additional line broadening which is angular dependent. In Fig. 1(b), the measurements of the angular dependence of the linewidth are shown; notice that a maximum occurs at 45° . Analyzing the linewidth data as outlined below, we have determined the degree of alignment for sample *A*.

The effect of the *c*-axis distribution on the linewidth is calculated as a function of angle θ between the magnetic

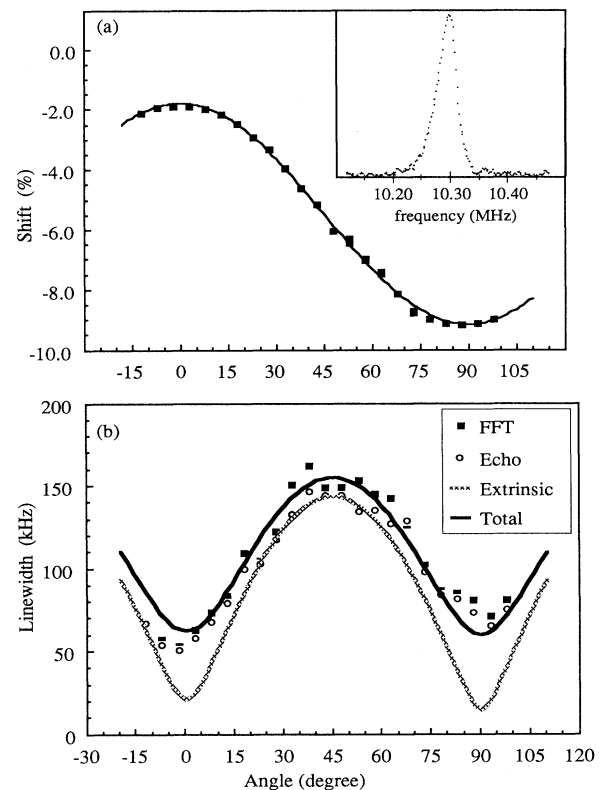


FIG. 1. (a) The angular dependence of the ^{195}Pt NMR shift at 4.94 K. The line is a fit to Eq. (1). Inset: the ^{195}Pt NMR magnitude spectrum at 4.94 K and 12.46 kG for $H \perp c$. The linewidth is 50 kHz. (b) The angular dependence of the linewidth (FWHM). The linewidth was measured from a fit to the spin echo (open circles) and a Fourier transform spectrum (filled squares). The light line indicates the contribution from misalignment and the dark line is the fit to the total linewidth discussed in the text.

field and the average c axis of the whiskers. Let ψ and φ be the polar and the azimuthal angles of the c axis of each whisker with respect to the average c axis of the ensemble of whiskers. Also let Φ be the angle between the field and the c axis of each whisker. Then, $\cos\Phi = -\sin\theta\sin\psi\sin\varphi + \cos\theta\cos\psi$. The ^{195}Pt resonance frequency of a whisker at the angle Φ in a fixed magnetic field, $\omega(\Phi)$, is determined by Eq. (1). The second moment of the linewidth is

$$\Delta\omega^2 \equiv \langle \omega^2 \rangle - \langle \omega \rangle^2 = A^2 [\langle \cos^4\Phi \rangle - \langle \cos^2\Phi \rangle^2],$$

where $A = K_{\parallel} - K_{\perp}$ and $\langle \dots \rangle$ is an average over ψ and φ for a specific distribution function describing the c -axis orientation. The average over φ is easily performed assuming a random distribution. For the average over ψ , we choose, for convenience, the Onsager distribution¹⁶ for the probability density P for the c axis at angle ψ ,

$$P(\psi) \propto \cosh(\alpha \cos\psi). \quad (2)$$

Here α is a constant determining the half-width of the distribution, $\psi_{1/2} = \cos^{-1}[1 - \ln(2)/\alpha]$. Then, the linewidth can be expressed analytically as a function of θ with the parameter α . In addition to this extrinsic effect, we also include an intrinsic contribution to the second moment, $(\Delta\omega_{\text{int}}^2)^{1/2}$, which, for example, comes from the ^{195}Pt nuclear spin-spin coupling and lifetime broadening. The total linewidth (FWHM) is defined as $\Delta\omega_{\text{total}} = 2.36(\Delta\omega_{\text{int}}^2 + \Delta\omega^2)^{1/2}$. We obtained a fit to the angular dependence of total linewidth with two parameters: $\psi_{1/2} = 5^\circ$ and $(\Delta\omega_{\text{int}}^2)^{1/2} = 25$ kHz. This narrow half-width for $\psi_{1/2}$ demonstrates the high degree of alignment obtained by our technique. For sample *B*, which was manually aligned and for which the alignment is considered to be better, the linewidth for $H\perp c$ was found to be similar to that of sample *A* at $H\perp c$. This indicates that for $H\perp c$, most of the contribution to the linewidth comes from the intrinsic width and not from imperfect alignment. The intrinsic width we have obtained is very large compared with the Van Vleck second moment¹⁷ due to nuclear dipole-dipole interactions, ~ 0.3 kHz. Therefore, the linewidth must be determined by other mechanisms. As we will show later, this is largely due to the extremely fast spin-lattice relaxation rate $1/T_1$, the so-called lifetime broadening effect.

IV. KNIGHT SHIFT AND SPIN-LATTICE RELAXATION

In Fig. 2, we show the temperature dependence of ^{195}Pt Knight shifts for $H\parallel c$ and $H\perp c$. The shifts are negative, indicative of the core polarization process¹⁸ which is typical of metals with unfilled d orbitals where d electrons polarize the core s electrons. The large magnitude of the shift is due to the large effective mass of the conduction electrons. The Knight shift is strongly temperature dependent for $H\perp c$ and $H\parallel c$. Our measurements of K and its temperature dependence are consistent with the powder results of Kohori and co-workers,^{14,19} but much more accurate due to the narrow linewidth of our spectra.

Contributions to the ^{195}Pt Knight shift can come from

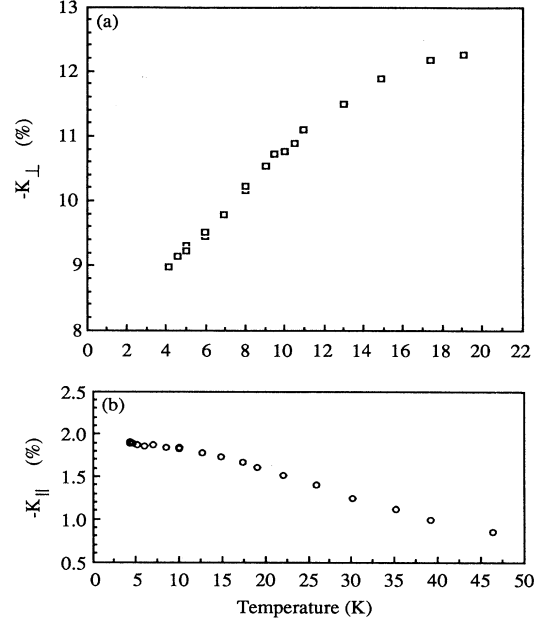


FIG. 2. The temperature dependence of ^{195}Pt NMR shift for (a) $H\perp c$ and (b) $H\parallel c$. The NMR frequency was fixed at 11 MHz.

both spin and orbital interactions with the conduction electrons: $K_{\perp\parallel} = K_{\perp\parallel}^s + K_{\perp\parallel}^{\text{orb}} = A_{\perp\parallel}^s \chi_{\perp\parallel}^s + A_{\perp\parallel}^{\text{orb}} \chi_{\perp\parallel}^{\text{orb}}$, where $K_{\perp\parallel}^s$ and $K_{\perp\parallel}^{\text{orb}}$ are the spin and orbital shifts, and $A_{\perp\parallel}^s$ and $A_{\perp\parallel}^{\text{orb}}$ are the corresponding hyperfine fields. The orbital shift depends on orbital currents and scales with the Val Vleck orbital paramagnetism.¹⁷ It is usually small, positive, and independent of temperature. The temperature dependence of the measured shifts is very similar to that of the dc susceptibility.¹⁵ In Figs. 3(a) and 3(b), we show a plot of K_{\parallel} and K_{\perp} vs χ with temperature as an implicit variable. Data for the dc susceptibility is taken from Ref. 15. The data points fall on straight lines indicating well-defined hyperfine fields and that the orbital shift is a constant within this temperature range. Thus the temperature dependence of K_{\parallel} and K_{\perp} comes from the spin degrees of freedom. Kohori *et al.*¹⁹ have found that the Pt Knight shift for $H\perp c$ is proportional to the dc magnetic susceptibility up to 150 K. For comparison, these results from Kohori *et al.*¹⁹ are shown as dashed lines in Fig. 3(a). With the high precision of our shift data for both orientations, we determine A_{\parallel}^s and A_{\perp}^s from the slopes:

$$A_{\parallel}^s = -69 \text{ kOe}/\mu_B, \quad A_{\perp}^s = -92 \text{ kOe}/\mu_B \quad (3)$$

showing a small but significant anisotropy in the hyperfine field.

However, the orbital shift, $K_{\perp\parallel}^{\text{orb}}$ cannot be obtained from such an analysis without an independent determination of $\chi_{\perp\parallel}^{\text{orb}}$. Since the values of $K_{\perp\parallel}^{\text{orb}}$ are important in the interpretation of the spin-lattice relaxation rates, we try to set a bound on $K_{\perp\parallel}^{\text{orb}}$. Due to the large effective mass of the conduction electrons, the dc susceptibility is dominated by contributions from the spin degrees of freedom and the orbital contribution is relatively small and can be

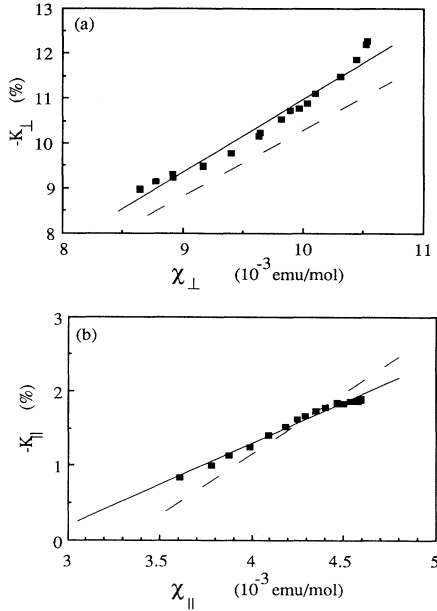


FIG. 3. The Knight shift vs dc magnetic susceptibility with temperature as an implicit parameter. (a) $H \perp c$ and (b) $H \parallel c$, respectively. The slopes of the fits (solid lines) determine the hyperfine coupling constants, and the dashed lines are from Ref. 19.

neglected. Hence, the ordinate intercept of the linear fit in the K - χ plot provides an estimate of the orbital shift, from which we find $K_{\parallel}^{\text{orb}} = 3.5\%$, and $K_{\perp}^{\text{orb}} = 5.5\%$. If the orbital susceptibility is considered then these values are nonzero bounds for the orbital shifts.

Spin-spin and spin-lattice relaxation rates were measured and the results are shown in Fig. 4. Both relaxation processes were found to be exponential for up to two decades of change in signal amplitude. For the temperatures explored, we found $1/T_2$ to be essentially temperature independent for both orientations. We found $1/T_1$

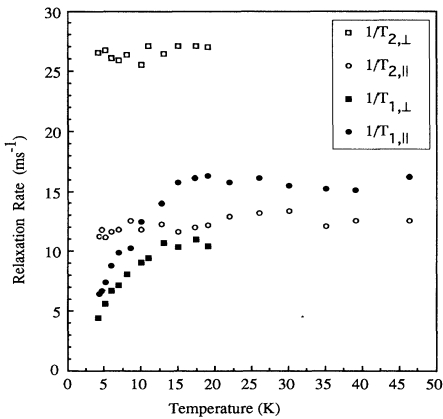


FIG. 4. The ^{195}Pt nuclear spin-spin ($1/T_2$) and spin-lattice ($1/T_1$) relaxation rates as a function of temperature for $H \perp c$ and $H \parallel c$.

also to be independent of temperature above 20 K and to decrease linearly with decreasing temperatures below 8 K. We were particularly careful to explore the region near 5 K to search for signatures of the AFM ordering indicated by neutron-scattering experiments.⁵ In this section, we focus on the temperature dependence of $1/T_1$ and the Knight shift. Discussion of $1/T_2$ will be found in Sec. V.

In Fig. 5, we show the temperature dependence of the anisotropy ratio of $1/T_1$ and $1/T_2$. These ratios are found to be independent of temperature for the temperature range 4–20 K. Our anisotropy ratio of 1.4 for $1/T_1$ is consistent with that by Vithayathil *et al.*²⁰ measured for temperatures below 4 K. If we are to neglect the q dependence of the hyperfine coupling, the anisotropy of the spin-lattice relaxation rate is given by

$$T_{1,\perp}/T_{1,\parallel} = 2A_{\perp}^2\chi'' / (A_{\perp}^2\chi'' + A_{\parallel}^2\chi'') = 1.4,$$

where χ'' is the imaginary part of the dynamic susceptibility at the NMR frequency. Therefore, $\chi''_{\perp}/\chi''_{\parallel} = 1.3$, taking into account anisotropy in the hyperfine field. This indicates that magnetic fluctuations are slightly stronger in the basal plane.

The nuclear spin-lattice-relaxation rates measure the imaginary part of the dynamic spin susceptibility at the Larmor frequency averaged over momentum space. Within a free-electron model, $T_1 T$ and K are constant in temperature. The product $T_1 T K^2$ is called the Korringa product, given by $\xi_0 = (\gamma_e/\gamma_n)^2 \hbar / (4\pi k_B)$, where γ_e and γ_n are the gyromagnetic ratios of electron and nucleus, respectively, \hbar the Planck constant, and k_B the Boltzmann constant. Deviations of $\xi \equiv T_1 T K^2$ from ξ_0 , are known to come from electron correlations and other many-body effects. For uniaxial anisotropy, two such products should be considered:²⁰

$$\begin{aligned} \xi_{\perp} &= K_{\perp}^2 T_{1,\parallel} T, \\ \xi_{\parallel} &= K_{\parallel}^2 T (2T_{1,\perp}^{-1} - T_{1,\parallel}^{-1})^{-1}. \end{aligned} \quad (4)$$

They separately measure the longitudinal and the transverse components of the dynamic susceptibility. A plot of ξ_{\perp} and ξ_{\parallel} is shown in Fig. 6. Data for K_{\perp} above 20 K

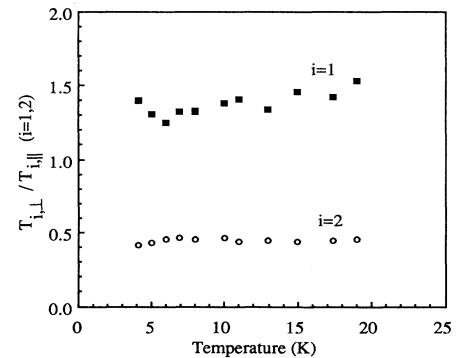


FIG. 5. The measured anisotropy of the relaxation rates, $T_{1,\perp}/T_{1,\parallel}$ (squares) and $T_{2,\perp}/T_{2,\parallel}$ (circles), as a function of temperature.

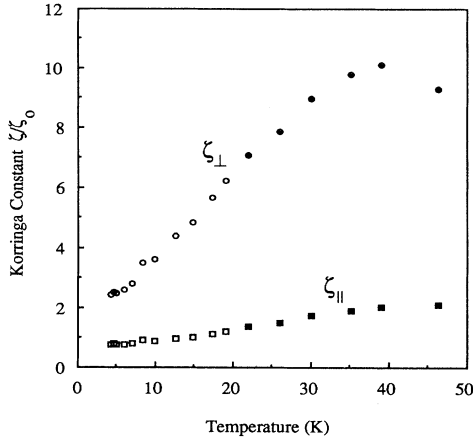


FIG. 6. Temperature dependence of Korrington constants: $\zeta_{\parallel}/\zeta_0$ (squares) and ζ_{\perp}/ζ_0 (circles). Data for K_{\perp} being used in ζ_{\perp}/ζ_0 above 20 K (closed circles) are obtained using the susceptibility data and the hyperfine coupling constant. $\zeta_{\parallel}/\zeta_0$ above 20 K (closed squares) are obtained assuming the same anisotropy ratio of $1/T_1$ as below 20 K.

was obtained from the susceptibility data and our hyperfine coupling constants. The data for ζ_{\parallel} are extended to 50 K by assuming the same constant anisotropy ratio of $1/T_1$ from 20–50 K. In making this plot, orbital shifts for both orientations are accounted for and the nonzero value of K^{orb} affects the Korrington products significantly for both ζ_{\perp} and ζ_{\parallel} . If we were to choose $K_{\parallel}^{\text{orb}}=0\%$ (or $K_{\perp}^{\text{orb}}=0\%$), ζ_{\parallel} (or ζ_{\perp}) would be reduced by a factor of 5 (or 2–3). However, the overall temperature dependence remains unchanged.

From Fig. 6, ζ_{\perp} is found to be strongly temperature dependent. It increases as the temperature increases and shows a maximum at 40 K and then decreases at higher temperature. On the other hand, ζ_{\parallel} is only weakly temperature dependent and increases slightly as the temperature increases. It is worth noting that the extrapolations of ζ_{\perp} and ζ_{\parallel} to zero temperature are very close to ζ_0 , the value expected for a simple metal.

The spin fluctuations are important in the crossover process from paramagnetic to a coherent Fermi liquid. Neutron-scattering experiments⁵ have indicated antiferromagnetic fluctuations of energy ~ 1 meV below 20 K in UPt_3 . These measurements⁵ have shown that the fluctuations increase as temperature is lowered and that antiferromagnetic order forms at 5 K. Such fluctuations, for example, the antiferromagnetic fluctuations at $Q_{\text{AF}}=(1/2,0,1)$, directly enhance the dynamical susceptibility at nonzero Q and hence reduce the Korrington product. The observed temperature dependence of ζ_{\parallel} and ζ_{\perp} , shown in Fig. 6, is consistent with this idea suggesting that spin fluctuations are responsible for the low-energy magnetic properties in this temperature range.

It has been argued²¹ that the temperature dependence of $1/T_1$ suggests a crossover from the degenerate Fermi-liquid regime below 8 K, $T_1 T = \text{const}$, to an incoherent spin fluctuation regime at higher temperature. However, this is not the correct picture since the Knight shift de-

pends strongly on temperature. The temperature dependence of both the Knight shift and T_1 must be taken into consideration, as expressed in the Korrington products ζ_{\parallel} and ζ_{\perp} . In Fig. 6, it is evident that ζ_{\perp} and ζ_{\parallel} vary monotonically in the region of 20 K indicating that this process is a continuous one, starting from 40–50 K. The peak in the Knight shift and susceptibility at 20 K results from a trade off between two effects: uncorrelated local moment paramagnetism at high temperature and the development of antiferromagnetic correlations at low temperature. They are of opposite sign, balancing one another around 20 K which should not be considered as an indication of a phase transition or the onset of a spin-fluctuation regime.

V. SPIN-SPIN RELAXATION RATES

The spin-spin relaxation rate was found to be extremely fast for both orientations largely due to lifetime broadening. For comparison, T_2 determined from the homonuclear dipolar interaction, is around 800 μs , much larger than the measured values and in fact can be neglected. For the field parallel to the average c axis, $1/T_2$ was smaller than $1/T_1$. This is unusual and is the result of anisotropy in $1/T_1$. According to the Redfield theory,¹⁷ contributions to $1/T_2$ from a randomly fluctuating field h with a correlation time τ are given by

$$1/T_{2R,\parallel} = \gamma_n^2 \overline{h_{\parallel}^2} \tau + 1/2T_{1,\parallel} = 1/T_{1,\perp}, \quad (5)$$

$$1/T_{2R,\perp} = \gamma_n^2 \overline{h_{\perp}^2} \tau + 1/2T_{1,\perp} = 1/2T_{1,\parallel} + 1/2T_{1,\perp}, \quad (6)$$

where $\overline{h^2}$ is the mean square average of the fluctuating local field. The second equality in each of Eqs. (5) and (6) is obtained assuming the correlation time τ much shorter than the Larmor period, i.e., $\omega_n \tau \ll 1$. From Fig. 4, we have found that $1/T_{2,\parallel}$ is slightly enhanced from that of Eq. (5) above 15 K, while $1/T_{2,\perp}$ is much larger than the value given by Eq. (6). There are two possibilities for this to occur. One is that $\omega_n \tau$ is of order 1; or there are additional contributions from other relaxation mechanisms. If $\omega_n \tau \sim 1$, $1/T_1$ and $1/T_2$ should be field dependent. We checked this possibility by comparing with the measurements at around 0.25 T by Kohori *et al.*²¹ The two results are in good agreement with each other. This rules out the possibility of $\omega_n \tau \sim 1$ and indicates that other mechanisms dominate the enhanced relaxation rate $1/T_{2,\perp}$. We can remove the Redfield contributions and the enhancement, $1/T_{2i} \equiv 1/T_2 - 1/T_{2R}$, for both orientations is shown in Fig. 7. An increase in $1/T_{2i}$ below 20 K is evident.

An indirect coupling, such as a nuclear spin-spin coupling mediated by electronic interactions, might be responsible for this enhancement. Such effects have been discussed recently in the context of $\text{YBa}_2\text{Cu}_3\text{O}_7$,²² where the indirect coupling between copper nuclear spins in the copper oxygen plane is believed to be strong. Should this be the case in UPt_3 , the anisotropy of this enhancement to $1/T_2$ indicates that this indirect coupling is strongly in the basal plane. The origin of this coupling might be related to the development of the AFM spin fluctuations

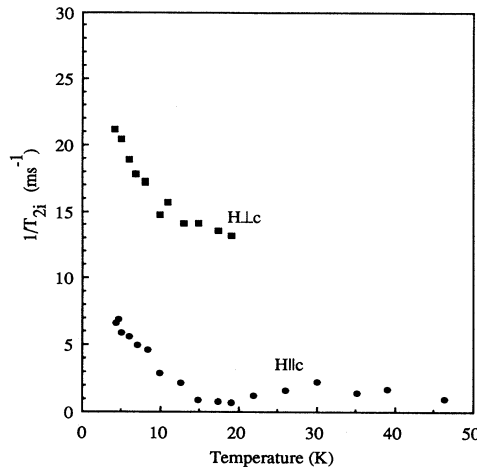


FIG. 7. Enhancement to $1/T_2$ given as $1/T_{2i} = 1/T_2 - 1/T_{2R}$, found by subtraction of lifetime broadening: $H_{\perp c}$ (squares) and $H_{\parallel c}$ (circles).

discussed earlier. However, we would like to be cautious about interpretation of the temperature dependence shown in Fig. 7 which is mainly derived from subtracting the Redfield contribution from an otherwise temperature independent T_2 .

Lastly, we discuss the antiferromagnetic ordering at 5 K, as observed in inelastic neutron scattering experiments.⁵ Usually, antiferromagnetic ordering is signaled by an abrupt change in the Knight shift or linewidth due to the presence of a static internal field, and possibly $1/T_1$ and $1/T_2$, due to the slowing down of magnetic fluctuations. We do not observe any significant change in Knight shift, linewidth, or $1/T_1$. Kohori *et al.*¹⁹ recently studied this problem by comparing the ^{195}Pt spectra in $\text{U}(\text{Pt}_{0.95}\text{Pd}_{0.05})_3$ and UPt_3 . The antiferromagnetic ordering in $\text{U}(\text{Pt}_{0.95}\text{Pd}_{0.05})_3$ broadens the ^{195}Pt resonance line and the internal field at the Pt site was determined to be 30 kOe. Comparing the ordered moments of $0.02\mu_B/\text{U}$ in UPt_3 (Ref. 5) and $0.65\mu_B/\text{U}$ in $\text{U}(\text{Pt}_{0.95}\text{Pd}_{0.05})_3$ (Ref.

23) and assuming the same spin structure, they estimated that the internal field in UPt_3 at the platinum site would be 900 Oe attributed to such ordering. They observed at most a small additional broadening of 10 Oe (Ref. 24) which appears to be inconsistent with static magnetic order. It is likely that the static magnetic order observed in neutron scattering is in fact fluctuations with a longer correlation time than the time scale of the neutron experiment but still much shorter than the NMR time scale.

VI. SUMMARY

We have developed a special technique for the alignment of the c axis of UPt_3 single-crystal whiskers so that the complete angular dependence of the Knight shift and relaxation rates can be studied. We report measurements of the ^{195}Pt Knight shift, spin-lattice and spin-spin relaxation rates in the temperature range of 4–50 K. We have determined the anisotropic hyperfine coupling constants parallel and perpendicular to the c axis. The Korringa products, appropriate for the anisotropic case, show a continuous evolution from a randomly fluctuating paramagnetic regime above 40 K to a degenerate Fermi-liquid behavior below 5 K. We argue that the low-energy antiferromagnetic spin fluctuations dominate both Knight shift and relaxation rates. The anisotropy of T_1 and T_2 is found to be 1.4 and 0.45, respectively, and temperature independent. Analyzing these anisotropy ratios, we find that the dynamic spin susceptibility is 30% larger in the basal plane.

ACKNOWLEDGMENTS

We thank Dr. J. Sauls and Dr. A. Garg at Northwestern University for valuable discussions about this subject. This work was supported by the NSF Low Temperature Physics Program, Grant No. DMR-9006338, by the MRL program of the NSF at the Materials Research Center of Northwestern University under Award No. DMR-9120521, and by the Department of Energy, Grant No. DE:FG05-86ER45268.

*Present address: Department of Physics, Kon-kuk University, Seoul, Korea.

¹For review, see Z. Fisk, D. W. Hess, C. J. Pethick, D. Pines, J. L. Smith, J. D. Thompson, and J. O. Willis, *Science* **239**, 33 (1988).

²G. R. Stewart, *Rev. Mod. Phys.* **56**, 755 (1984); G. R. Stewart, *J. Appl. Phys.* **57**, 3049 (1985).

³A. de Visser, A. Menovsky, and J. J. M. Franse, *Physica B* **147**, 81 (1987).

⁴U. Rauchschwalbe, *Physica B* **147**, 1 (1987).

⁵G. Aeppli, E. Bucher, C. Broholm, J. K. Kjems, J. Baumann, and J. Hufnagl, *Phys. Rev. Lett.* **60**, 615 (1988); G. Aeppli, D. Bishop, C. Broholm, E. Bucher, K. Siemensmeyer, M. Steiner, and N. Stüsser, *ibid.* **63**, 676 (1989).

⁶G. Aeppli, E. Bucher, and G. Shirane, *Phys. Rev. B* **32**, 7579 (1985); G. Aeppli, A. Goldman, G. Shirane, E. Bucher, and M.-Ch. Lux-Steiner, *Phys. Rev. Lett.* **58**, 808 (1987).

⁷A. I. Goldman, G. Shirane, G. Aeppli, E. Bucher, and J. Hufnagl, *Phys. Rev. B* **36**, 8523 (1987); G. Aeppli, E. Bucher, A. I. Goldman, G. Shirane, C. Broholm, and J. K. Kjems, *J. Magn. Magn. Mater.* **76-77**, 385 (1988); G. Aeppli, C. Broholm, E. Bucher, and D. J. Bishop, *Physica B* **171**, 278 (1991).

⁸S. M. Hayden, L. Taillefer, C. Vettier, and J. Flouquet, *Phys. Rev. B* **46**, 8675 (1992); R. Joynt, *Supercon. Sci. Tech.* **1**, 210 (1988); D. W. Hess, T. A. Tokuyasu, and J. A. Sauls, *J. Phys. Cond. Mater.* **1**, 8135 (1989).

⁹D. E. MacLaughlin, C. Tien, W. G. Clark, M. D. Lan, Z. Fisk, J. L. Smith, and H. R. Ott, *Phys. Rev. Lett.* **53**, 1833 (1984); W. G. Clark, M. D. Lan, G. van Kelkeren, W. H. Wong, C. Tien, D. E. MacLaughlin, J. L. Smith, Z. Fisk, and H. R. Ott, *J. Magn. Magn. Mater.* **63-64**, 396 (1987); K. Asayama, Y. Kitaoka, and Y. Kohori, *ibid.* **76-77**, 449 (1988); H. Nakamura, Y. Kitaoka, K. Asayama, and J. Flouquet, *ibid.* **76-77**, 465

- (1988).
- ¹⁰D. E. MacLaughlin, *J. Magn. Magn. Mater.* **47-48**, 121 (1985).
- ¹¹A. A. V. Gibson, J. R. Owers-Bradley, I. D. Calder, J. B. Ketterson, and W. P. Halperin, *Rev. Sci. Instr.* **52**, 1509 (1981).
- ¹²C. H. Pennington, Ph.D. thesis, University of Illinois at Urbana-Champaign, 1989 (unpublished).
- ¹³G. C. Carter, L. H. Bennett, and D. J. Kahan, *Prog. Mater. Sci.* **20**, 295 (1977).
- ¹⁴Y. Kohori, T. Kohara, H. Shibai, Y. Oda, T. Kaneko, Y. Kitaoka, and K. Asayama, *J. Phys. Soc. Jpn.* **56**, 2263 (1987).
- ¹⁵W. D. Schneider and C. Laubschat, *Phys. Rev. B* **23**, 997 (1981); J. J. M. Franse, A. de Visser, A. Menovsky, and P. H. Frings, *J. Magn. Magn. Mater.* **52**, 61 (1985); A. de Visser, A. Menovsky, and J. J. M. Franse, *ibid.* **63-64**, 365 (1987).
- ¹⁶P. D. de Gennes, *The Physics of Liquid Crystals* (Oxford University Press, Oxford, 1974).
- ¹⁷C. P. Slichter, *Principles of Magnetic Resonances*, 3rd ed. (Springer-Verlag, Berlin, 1990).
- ¹⁸R. Kubo and Y. Obata, *J. Phys. Soc. Jpn.* **11**, 547 (1956).
- ¹⁹Y. Kohori, M. Kyogaku, T. Kohara, K. Asayama, H. Amitsuka, and Y. Miyako, *J. Magn. Magn. Mater.* **90-91**, 510 (1990).
- ²⁰J. P. Vithayathil, D. E. MacLaughlin, E. Koster, D. L. Williams, and E. Bucher, *Phys. Rev. B* **44**, 4705 (1991).
- ²¹Y. Kohori, T. Kohara, H. Shibai, Y. Oda, Y. Kitaoka, and K. Asayama, *J. Phys. Soc. Jpn.* **57**, 395 (1988); Y. Kohori, M. Kyogaku, T. Kohara, K. Asayama, H. Amitsuka, and Y. Miyako, *Physica B* **165-166**, 381 (1990).
- ²²C. H. Pennington *et al.*, *Phys. Rev. B* **39**, 274 (1989); Y.-Q. Song and W. P. Halperin, *Physica C* **191**, 131 (1992).
- ²³A. I. Goldman, G. Shirane, G. Aeppli, B. Batlogg, and E. Bucher, *Phys. Rev. B* **34**, 6564 (1986).
- ²⁴K. Asayama, Y. Kitaoka, and Y. Kohori, *Physica B* **171**, 226 (1991).